# Measurements of the branching fractions of the singly Cabibbo-suppressed decays $D^0 \to \omega\eta$, $\eta^{(\prime)}\pi^0$ and $\eta^{(\prime)}\eta$

M. Ablikim,[1] M. N. Achasov,[9,d] S. Ahmed,[14] O. Albayrak,[5] M. Albrecht,[4] D. J. Ambrose,[46] A. Amoroso,[51a,51c] F. F. An,[1] Q. An,[48,39] J. Z. Bai,[1] O. Bakina,[24] R. Baldini Ferroli,[20a] Y. Ban,[32] D. W. Bennett,[19] J. V. Bennett,[5] N. Berger,[23] M. Bertani,[20a] D. Bettoni,[21a] J. M. Bian,[45] F. Bianchi,[51a,51c] E. Boger,[24,b] I. Boyko,[24] R. A. Briere,[5] H. Cai,[53] X. Cai,[1,39] O. Cakir,[42a] A. Calcaterra,[20a] G. F. Cao,[1,43] S. A. Cetin,[42b] J. Chai,[51c] J. F. Chang,[1,39] G. Chelkov,[24,b,c] G. Chen,[1] H. S. Chen,[1,43] J. C. Chen,[1] M. L. Chen,[1,39] P. L. Chen,[49] S. J. Chen,[30] X. R. Chen,[27] Y. B. Chen,[1,39] X. K. Chu,[32] G. Cibinetto,[21a] H. L. Dai,[1,39] J. P. Dai,[35,h] A. Dbeyssi,[14] D. Dedovich,[24] Z. Y. Deng,[1] A. Denig,[23] I. Denysenko,[24] M. Destefanis,[51a,51c] F. De Mori,[51a,51c] Y. Ding,[28] C. Dong,[31] J. Dong,[1,39] L. Y. Dong,[1,43] M. Y. Dong,[1,39,43] Z. L. Dou,[30] S. X. Du,[55] P. F. Duan,[1] J. Fang,[1,39] S. S. Fang,[1,43] X. Fang,[48,39] Y. Fang,[1] R. Farinelli,[21a,21b] L. Fava,[51b,51c] S. Fegan,[23] F. Feldbauer,[23] G. Felici,[20a] C. Q. Feng,[48,39] E. Fioravanti,[21a] M. Fritsch,[23,14] C. D. Fu,[1] Q. Gao,[1] X. L. Gao,[48,39] Y. Gao,[41] Y. G. Gao,[6] Z. Gao,[48,39] I. Garzia,[21a] K. Goetzen,[10] L. Gong,[31] W. X. Gong,[1,39] W. Gradl,[23] M. Greco,[51a,51c] M. H. Gu,[1,39] S. Gu,[15] Y. T. Gu,[12] A. Q. Guo,[1] L. B. Guo,[29] R. P. Guo,[1,43] Y. P. Guo,[23] Z. Haddadi,[26] A. Hafner,[23] S. Han,[53] X. Q. Hao,[15] F. A. Harris,[44] K. L. He,[1,43] X. Q. He,[47] F. H. Heinsius,[4] T. Held,[4] Y. K. Heng,[1,39,43] T. Holtmann,[4] Z. L. Hou,[1] C. Hu,[29] H. M. Hu,[1,43] T. Hu,[1,39,43] Y. Hu,[1] G. S. Huang,[48,39] J. S. Huang,[15] X. T. Huang,[34] X. Z. Huang,[30] Z. L. Huang,[28] T. Hussain,[50] W. Ikegami Andersson,[52] Q. Ji,[1] Q. P. Ji,[15] X. B. Ji,[1,43] X. L. Ji,[1,39] X. S. Jiang,[1,39,43] X. Y. Jiang,[31] J. B. Jiao,[34] Z. Jiao,[17] D. P. Jin,[1,39,43] S. Jin,[1,43] T. Johansson,[52] A. Julin,[45] N. Kalantar-Nayestanaki,[26] X. L. Kang,[1] X. S. Kang,[31] M. Kavatsyuk,[26] B. C. Ke,[5] T. Khan,[48,39] P. Kiese,[23] R. Kliemt,[10] B. Kloss,[23] O. B. Kolcu,[42b,f] B. Kopf,[4] M. Kornicer,[44] A. Kupsc,[52] W. Kühn,[25] J. S. Lange,[25] M. Lara,[19] P. Larin,[14] L. Lavezzi,[51c] H. Leithoff,[23] C. Leng,[51c] C. Li,[52] Cheng Li,[48,39] D. M. Li,[55] F. Li,[1,39] F. Y. Li,[32] G. Li,[1] H. B. Li,[1,43] H. J. Li,[1,43] J. C. Li,[1] Jin Li,[33] Kang Li,[13] Ke Li,[34] Lei Li,[3] P. L. Li,[48,39] P. R. Li,[43,7] Q. Y. Li,[34] T. Li,[34] W. D. Li,[1,43] W. G. Li,[1] X. L. Li,[34] X. N. Li,[1,39] X. Q. Li,[31] Z. B. Li,[40] H. Liang,[48,39] Y. F. Liang,[37] Y. T. Liang,[25] G. R. Liao,[11] D. X. Lin,[14] B. Liu,[35,h] B. J. Liu,[1] C. X. Liu,[1] D. Liu,[48,39] F. H. Liu,[36] Fang Liu,[1] Feng Liu,[6] H. B. Liu,[12] H. M. Liu,[1,43] Huanhuan Liu,[1] Huihui Liu,[16] J. B. Liu,[48,39] J. P. Liu,[53] J. Y. Liu,[1,43] K. Liu,[41] K. Y. Liu,[28] Ke Liu,[6] L. D. Liu,[32] P. L. Liu,[1,39] Q. Liu,[43] S. B. Liu,[48,39] X. Liu,[27] Y. B. Liu,[31] Z. A. Liu,[1,39,43] Zhiqing Liu,[23] H. Loehner,[26] Y. F. Long,[32] X. C. Lou,[1,39,43] H. J. Lu,[17] J. G. Lu,[1,39] Y. Lu,[1] Y. P. Lu,[1,39] C. L. Luo,[29] M. X. Luo,[54] T. Luo,[44] X. L. Luo,[1,39] X. R. Lyu,[43] F. C. Ma,[28] H. L. Ma,[1] L. L. Ma,[34] M. M. Ma,[1,43] Q. M. Ma,[1] T. Ma,[1] X. N. Ma,[31] X. Y. Ma,[1,39] Y. M. Ma,[34] F. E. Maas,[14] M. Maggiora,[51a,51c] Q. A. Malik,[50] Y. J. Mao,[32] Z. P. Mao,[1] S. Marcello,[51a,51c] J. G. Messchendorp,[26] G. Mezzadri,[21b] J. Min,[1,39] T. J. Min,[1] R. E. Mitchell,[19] X. H. Mo,[1,39,43] Y. J. Mo,[6] C. Morales Morales,[14] G. Morello,[20a] N. Yu. Muchnoi,[9,d] H. Muramatsu,[45] P. Musiol,[4] Y. Nefedov,[24] F. Nerling,[10] I. B. Nikolaev,[9,d] Z. Ning,[1,39] S. Nisar,[8] S. L. Niu,[1,39] X. Y. Niu,[1,43] S. L. Olsen,[33,j] Q. Ouyang,[1,39,43] S. Pacetti,[20b] Y. Pan,[48,39] M. Papenbrock,[52] P. Patteri,[20a] M. Pelizaeus,[4] J. Pellegrino,[51a,51c] H. P. Peng,[48,39] K. Peters,[10,g] J. Pettersson,[52] J. L. Ping,[29] R. G. Ping,[1,43] R. Poling,[45] V. Prasad,[48,39] H. R. Qi,[2] M. Qi,[30] S. Qian,[1,39] C. F. Qiao,[43] J. J. Qin,[43] N. Qin,[53] X. S. Qin,[1] Z. H. Qin,[1,39] J. F. Qiu,[1] K. H. Rashid,[50,i] C. F. Redmer,[23] M. Ripka,[23] G. Rong,[1,43] Ch. Rosner,[14] A. Sarantsev,[24,e] M. Savrié,[21b] C. Schnier,[4] K. Schoenning,[52] W. Shan,[32] M. Shao,[48,39] C. P. Shen,[2] P. X. Shen,[31] X. Y. Shen,[1,43] H. Y. Sheng,[1] J. J. Song,[34] W. M. Song,[34] X. Y. Song,[1] S. Sosio,[51a,51c] S. Spataro,[51a,51c] G. X. Sun,[1] J. F. Sun,[15] S. S. Sun,[1,43] X. H. Sun,[1] Y. J. Sun,[48,39] Y. K. Sun,[48,39] Y. Z. Sun,[1] Z. J. Sun,[1,39] Z. T. Sun,[19] C. J. Tang,[37] X. Tang,[1] I. Tapan,[42c] E. H. Thorndike,[46] M. Tiemens,[26] B. Tsednee,[22] I. Uman,[42d] G. S. Varner,[44] B. Wang,[1] B. L. Wang,[43] D. Wang,[32] D. Y. Wang,[32] Dan Wang,[43] K. Wang,[1,39] L. L. Wang,[1] L. S. Wang,[1] M. Wang,[34] Meng Wang,[1,43] P. Wang,[1] P. L. Wang,[1] W. P. Wang,[48,39] X. F. Wang,[41] Y. Wang,[38] Y. D. Wang,[14] Y. F. Wang,[1,39,43] Y. Q. Wang,[23] Z. Wang,[1,39] Z. G. Wang,[1,39] Z. H. Wang,[48,39] Z. Y. Wang,[1] Zongyuan Wang,[1,43] T. Weber,[23] D. H. Wei,[11] P. Weidenkaff,[23] S. P. Wen,[1] U. Wiedner,[4] M. Wolke,[52] L. H. Wu,[1] L. J. Wu,[1,43] Z. Wu,[1,39] L. Xia,[48,39] Y. Xia,[18] D. Xiao,[1] H. Xiao,[49] Y. J. Xiao,[1,43] Z. J. Xiao,[29] Y. G. Xie,[1,39] Y. H. Xie,[6] X. A. Xiong,[1,43] Q. L. Xiu,[1,39] G. F. Xu,[1] J. J. Xu,[1,43] L. Xu,[1] Q. J. Xu,[13] Q. N. Xu,[43] X. P. Xu,[38] L. Yan,[51a,51c] W. B. Yan,[48,39] W. C. Yan,[48,39] Y. H. Yan,[18] H. J. Yang,[35,h] H. X. Yang,[1] L. Yang,[53] Y. H. Yang,[30] Y. X. Yang,[11] Yifan Yang,[1,43] M. Ye,[1,39] M. H. Ye,[7] J. H. Yin,[1] Z. Y. You,[40] B. X. Yu,[1,39,43] C. X. Yu,[31] J. S. Yu,[27] C. Z. Yuan,[1,43] Y. Yuan,[1] A. Yuncu,[42b,a] A. A. Zafar,[50] A. Zallo,[20a] Y. Zeng,[18] Z. Zeng,[48,39] B. X. Zhang,[1] B. Y. Zhang,[1,39] C. C. Zhang,[1] D. H. Zhang,[1] H. H. Zhang,[40] H. Y. Zhang,[1,39] J. Zhang,[1,43] J. L. Zhang,[1] J. Q. Zhang,[1] J. W. Zhang,[1,39,43] J. Y. Zhang,[1] J. Z. Zhang,[1,43] K. Zhang,[1,43] L. Zhang,[41] S. Q. Zhang,[31] X. Y. Zhang,[34] Y. H. Zhang,[1,39] Y. T. Zhang,[48,39] Yang Zhang,[1] Yao Zhang,[1] Yu Zhang,[43] Z. H. Zhang,[6] Z. P. Zhang,[48] Z. Y. Zhang,[53] G. Zhao,[1] J. W. Zhao,[1,39] J. Y. Zhao,[1,43] J. Z. Zhao,[1,39] Lei Zhao,[48,39] Ling Zhao,[1] M. G. Zhao,[31] Q. Zhao,[1] S. J. Zhao,[55] T. C. Zhao,[1] Y. B. Zhao,[1,39] Z. G. Zhao,[48,39] A. Zhemchugov,[24,b] B. Zheng,[49] J. P. Zheng,[1,39] W. J. Zheng,[34] Y. H. Zheng,[43] B. Zhong,[29] L. Zhou,[1,39] X. Zhou,[53] X. K. Zhou,[48,39] X. R. Zhou,[48,39] X. Y. Zhou,[1] Y. X. Zhou,[12] J. Zhu,[31] K. Zhu,[1] K. J. Zhu,[1,39,43] S. Zhu,[1] S. H. Zhu,[47] X. L. Zhu,[41] Y. C. Zhu,[48,39] Y. S. Zhu,[1,43] Z. A. Zhu,[1,43] J. Zhuang,[1,39] L. Zotti,[51a,51c] B. S. Zou,[1] and J. H. Zou[1]

(BESIII Collaboration)

[1]*Institute of High Energy Physics, Beijing 100049, People's Republic of China*
[2]*Beihang University, Beijing 100191, People's Republic of China*
[3]*Beijing Institute of Petrochemical Technology, Beijing 102617, People's Republic of China*
[4]*Bochum Ruhr-University, D-44780 Bochum, Germany*
[5]*Carnegie Mellon University, Pittsburgh, Pennsylvania 15213, USA*
[6]*Central China Normal University, Wuhan 430079, People's Republic of China*
[7]*China Center of Advanced Science and Technology, Beijing 100190, People's Republic of China*
[8]*COMSATS Institute of Information Technology, Lahore, Defence Road, Off Raiwind Road, 54000 Lahore, Pakistan*
[9]*G.I. Budker Institute of Nuclear Physics SB RAS (BINP), Novosibirsk 630090, Russia*
[10]*GSI Helmholtzcentre for Heavy Ion Research GmbH, D-64291 Darmstadt, Germany*
[11]*Guangxi Normal University, Guilin 541004, People's Republic of China*
[12]*Guangxi University, Nanning 530004, People's Republic of China*
[13]*Hangzhou Normal University, Hangzhou 310036, People's Republic of China*
[14]*Helmholtz Institute Mainz, Johann-Joachim-Becher-Weg 45, D-55099 Mainz, Germany*
[15]*Henan Normal University, Xinxiang 453007, People's Republic of China*
[16]*Henan University of Science and Technology, Luoyang 471003, People's Republic of China*
[17]*Huangshan College, Huangshan 245000, People's Republic of China*
[18]*Hunan University, Changsha 410082, People's Republic of China*
[19]*Indiana University, Bloomington, Indiana 47405, USA*
[20a]*INFN Laboratori Nazionali di Frascati, I-00044 Frascati, Italy*
[20b]*INFN and University of Perugia, I-06100 Perugia, Italy*
[21a]*INFN Sezione di Ferrara, I-44122 Ferrara, Italy*
[21b]*University of Ferrara, I-44122 Ferrara, Italy*
[22]*Institute of Physics and Technology, Peace Ave. 54B, Ulaanbaatar 13330, Mongolia*
[23]*Johannes Gutenberg University of Mainz, Johann-Joachim-Becher-Weg 45, D-55099 Mainz, Germany*
[24]*Joint Institute for Nuclear Research, 141980 Dubna, Moscow region, Russia*
[25]*Justus-Liebig-Universitaet Giessen, II. Physikalisches Institut, Heinrich-Buff-Ring 16, D-35392 Giessen, Germany*
[26]*KVI-CART, University of Groningen, NL-9747 AA Groningen, The Netherlands*
[27]*Lanzhou University, Lanzhou 730000, People's Republic of China*
[28]*Liaoning University, Shenyang 110036, People's Republic of China*
[29]*Nanjing Normal University, Nanjing 210023, People's Republic of China*
[30]*Nanjing University, Nanjing 210093, People's Republic of China*
[31]*Nankai University, Tianjin 300071, People's Republic of China*
[32]*Peking University, Beijing 100871, People's Republic of China*
[33]*Seoul National University, Seoul 151-747, Korea*
[34]*Shandong University, Jinan 250100, People's Republic of China*
[35]*Shanghai Jiao Tong University, Shanghai 200240, People's Republic of China*
[36]*Shanxi University, Taiyuan 030006, People's Republic of China*
[37]*Sichuan University, Chengdu 610064, People's Republic of China*
[38]*Soochow University, Suzhou 215006, People's Republic of China*
[39]*State Key Laboratory of Particle Detection and Electronics, Beijing 100049, Hefei 230026, People's Republic of China*
[40]*Sun Yat-Sen University, Guangzhou 510275, People's Republic of China*
[41]*Tsinghua University, Beijing 100084, People's Republic of China*
[42a]*Ankara University, 06100 Tandogan, Ankara, Turkey*
[42b]*Istanbul Bilgi University, 34060 Eyup, Istanbul, Turkey*
[42c]*Uludag University, 16059 Bursa, Turkey*
[42d]*Near East University, Nicosia, North Cyprus, 33010 Mersin, Turkey*
[43]*University of Chinese Academy of Sciences, Beijing 100049, People's Republic of China*
[44]*University of Hawaii, Honolulu, Hawaii 96822, USA*
[45]*University of Minnesota, Minneapolis, Minnesota 55455, USA*
[46]*University of Rochester, Rochester, New York 14627, USA*
[47]*University of Science and Technology Liaoning, Anshan 114051, People's Republic of China*
[48]*University of Science and Technology of China, Hefei 230026, People's Republic of China*
[49]*University of South China, Hengyang 421001, People's Republic of China*

[50]University of the Punjab, Lahore-54590, Pakistan
[51a]University of Turin, I-10125 Turin, Italy
[51b]University of Eastern Piedmont, I-15121 Alessandria, Italy
[51c]INFN, I-10125 Turin, Italy
[52]Uppsala University, Box 516, SE-75120 Uppsala, Sweden
[53]Wuhan University, Wuhan 430072, People's Republic of China
[54]Zhejiang University, Hangzhou 310027, People's Republic of China
[55]Zhengzhou University, Zhengzhou 450001, People's Republic of China

(Received 18 January 2018; published 15 March 2018)

By analyzing a data sample of 2.93 $\text{fb}^{-1}$ collected at $\sqrt{s} = 3.773$ GeV with the BESIII detector operated at the BEPCII storage rings, we measure the branching fractions $\mathcal{B}(D^0 \to \omega\eta) = (2.15 \pm 0.17_{\text{stat}} \pm 0.15_{\text{sys}}) \times 10^{-3}$, $\mathcal{B}(D^0 \to \eta\pi^0) = (0.58 \pm 0.05_{\text{stat}} \pm 0.05_{\text{sys}}) \times 10^{-3}$, $\mathcal{B}(D^0 \to \eta'\pi^0) = (0.93 \pm 0.11_{\text{stat}} \pm 0.09_{\text{sys}}) \times 10^{-3}$, $\mathcal{B}(D^0 \to \eta\eta) = (2.20 \pm 0.07_{\text{stat}} \pm 0.06_{\text{sys}}) \times 10^{-3}$ and $\mathcal{B}(D^0 \to \eta'\eta) = (0.94 \pm 0.25_{\text{stat}} \pm 0.11_{\text{sys}}) \times 10^{-3}$. We note that $\mathcal{B}(D^0 \to \omega\eta)$ is measured for the first time and that $\mathcal{B}(D^0 \to \eta\eta)$ is measured with much improved precision.

DOI: 10.1103/PhysRevD.97.052005

## I. INTRODUCTION

Hadronic decays of charmed mesons open a window to explore the interplay between weak and strong interactions. Based on flavor SU(3) symmetry, different topological amplitudes for two-body hadronic decays of $D$ mesons can be extracted by diagrammatic approach [1–3] or factorization-assisted topological-amplitude approach [4]. Consequently, comprehensive measurements of their branching fractions (BFs) can not only test the theoretical calculations, but also shed light on the understanding of SU(3)-flavor symmetry-breaking effects in $D$ decays [5].

Two-body $D$ hadronic decays have been extensively investigated in previous experiments [6]. However, experimental knowledge of some singly Cabibbo-suppressed (SCS) decays involving four photons, e.g., $D^0 \to \omega\pi^0$, $\omega\eta$, $\pi^0\pi^0$, $\eta\pi^0$, $\eta'\pi^0$, $\eta\eta$ and $\eta'\eta$, is still poor due to low statistics and high backgrounds. The decay $D^0 \to \omega\eta$ is particularly interesting, since it only occurs via $W$-internal emission and $W$-exchange, as shown in Fig. 1, and its decay BF is expected to be at the $10^{-3}$ level [2]. However, it has not yet been measured in any experiment.

Previously, the CLEO Collaboration reported the measurements of the BFs of $D^0 \to \eta\pi^0$, $\eta\eta$, $\eta'\pi^0$, $\eta'\eta$ [7,8]. During 2010 and 2011, a data sample with an integrated luminosity of 2.93 $\text{fb}^{-1}$ [9] was collected with the BESIII detector at a center-of-mass energy $\sqrt{s} = 3.773$ GeV. In $e^+e^-$ annihilations at this energy, $D$ mesons are produced in pairs with no additional particles and can serve as an ideal test-bed to systematically study $D$ decays. With this data sample, the BFs of the two-body hadronic decays $D^0 \to \pi^0\pi^0$ [10] and $D^0 \to \omega\pi^0, \eta\pi^0$ [11] have been previously measured using single-tagged and double-tagged events, respectively, in which one and two $D$ mesons are reconstructed in each event. In this paper, we report the measurements of the BFs for $D^0 \to \omega\eta$, $\eta\pi^0$, $\eta'\pi^0$, $\eta\eta$ and $\eta'\eta$, by analyzing single-tag events using this data sample. Throughout this paper, the inclusion of charge-conjugate final states is implied.

## II. BESIII DETECTOR AND MONTE CARLO SIMULATION

The BESIII detector in Beijing, China, is a cylindrical detector with a solid-angle coverage of 93% of $4\pi$ that operates at the BEPCII collider consisting of the following five main components. A 43-layer main drift chamber

[a]Also at Bogazici University, 34342 Istanbul, Turkey.
[b]Also at the Moscow Institute of Physics and Technology, Moscow 141700, Russia.
[c]Also at the Functional Electronics Laboratory, Tomsk State University, Tomsk, 634050, Russia.
[d]Also at the Novosibirsk State University, Novosibirsk, 630090, Russia.
[e]Also at the NRC "Kurchatov Institute", PNPI, 188300, Gatchina, Russia.
[f]Also at Istanbul Arel University, 34295 Istanbul, Turkey.
[g]Also at Goethe University Frankfurt, 60323 Frankfurt am Main, Germany.
[h]Also at Key Laboratory for Particle Physics, Astrophysics and Cosmology, Ministry of Education; Shanghai Key Laboratory for Particle Physics and Cosmology; Institute of Nuclear and Particle Physics, Shanghai 200240, People's Republic of China.
[i]Government College Women University, Sialkot - 51310. Punjab, Pakistan.
[j]Present address: Center for Underground Physics, Institute for Basic Science, Daejeon 34126, Korea.

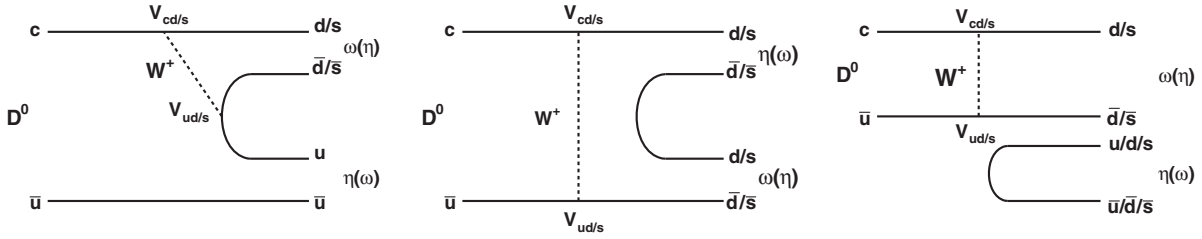


FIG. 1. The Feynman diagrams for the SCS decay $D^0 \to \omega\eta$.

(MDC) surrounding the beam pipe provides precise determinations of charged particle trajectories and ionization energy losses ($dE/dx$) for charged particle identification (PID). An array of time-of-flight counters (TOF) is located outside the MDC and provides additional information for PID. A CsI(Tl) electromagnetic calorimeter (EMC) surrounds the TOF and is used to measure energies of electromagnetic showers. A solenoidal superconducting magnet outside the EMC provides a 1 T magnetic field in the central tracking region of the detector. The iron flux return yoke of the magnet is instrumented with 1272 $m^2$ of resistive plate muon counters arranged in nine layers in the barrel and eight layers in the end-caps. More details of the BESIII detector are described in Ref. [12].

A GEANT4-based [13] Monte Carlo (MC) simulation software package, which includes the geometrical description of the detector and its response, is used to determine the detection efficiency and to estimate the potential backgrounds. An inclusive MC sample produced at $\sqrt{s} = 3.773$ GeV consists of $D^0\bar{D}^0$, $D^+D^-$ and non-$D\bar{D}$ decays of $\psi(3770)$, initial-state radiation (ISR) production of $\psi(3686)$ and $J/\psi$, the $q\bar{q}$ ($q = u, d, s$) continuum process, and Bhabha scattering, di-muon and di-tau events. The $\psi(3770)$ is generated by the MC generator KKMC [14], in which ISR effects [15] and final state radiation (FSR) effects [16] are considered. The known decay modes of $J/\psi$, $\psi(3686)$ and $\psi(3770)$ are generated by using BesEvtGen [17] with BFs quoted from the PDG [18], and the remaining events are generated with LundCharm [19]. The inclusive MC sample corresponds to about 10 times the equivalent luminosity of data. To determine reconstruction efficiencies, large exclusive MC samples ('signal MC') of 200 000 events per decay mode are used.

## III. DATA ANALYSIS

The two-body $D$ hadronic decays of interest are selected from combinations of $\pi^0$, $\eta$, $\omega$ and $\eta'$ mesons reconstructed using $\pi^0 \to \gamma\gamma$, $\eta \to \gamma\gamma$, $\omega \to \pi^+\pi^-\pi^0$ and $\eta' \to \pi^+\pi^-\eta$ decays, respectively. The $D^0 \to \eta\eta$ decay is also reconstructed using one $\eta$ undergoing a $\gamma\gamma$ decay and the other decaying to the $\pi^+\pi^-\pi^0$ final state. In the following, we use $\eta_\gamma$ and $\eta_\pi$ in the decay $D^0 \to \eta\eta$ to denote the decay modes $\eta \to \gamma\gamma$ and $\eta \to \pi^+\pi^-\pi^0$, respectively, but simply use $\eta$ for the other $D^0$ decays with a final-state $\eta$ to represent the decay $\eta \to \gamma\gamma$.

The minimum distance of a charged track to the interaction point (IP) is required to be within 10 cm along the beam direction and within 1 cm in the perpendicular plane. The polar angle $\theta$ of a charged track with respect to the positron beam direction is required satisfy $|\cos\theta| < 0.93$. PID is performed by using the $dE/dx$ and TOF measurements to calculate confidence levels for pion and kaon hypotheses, $CL_\pi$ and $CL_K$. Charged pions are required to satisfy $CL_\pi > CL_K$.

Photon candidates are chosen from isolated EMC clusters with energy larger than 25 (50) MeV if the crystal with the maximum deposited energy in that cluster is in the barrel (end-cap) region [12]. Clusters due to electronic noise or beam backgrounds are suppressed by requiring clusters to occur no later than 700 ns from the event start time. To reject photons from bremsstrahlung or from secondary interactions,

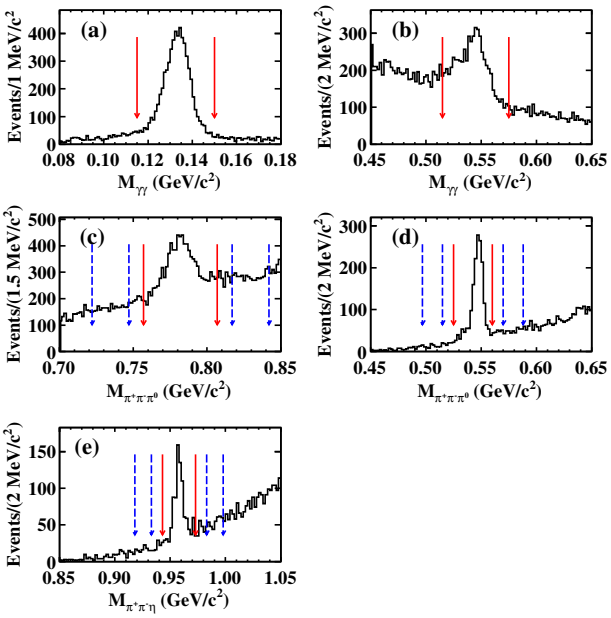


FIG. 2. Distributions of the invariant masses for (a, b) the $\gamma\gamma$ combinations from the $D^0 \to \eta\pi^0$ candidate events, (c, d) the $\pi^+\pi^-\pi^0$ combinations from the $D^0 \to \omega\eta$ and $D^0 \to \eta_\pi\eta_\gamma$ candidate events, (e) the $\pi^+\pi^-\eta$ combinations from the $D^0 \to \eta'\pi^0$ candidate events. The ranges between the red solid (blue dashed) arrows denote the corresponding signal (sideband) regions.

TABLE I. Signal and sideband regions for $\eta_\pi$, $\omega$ and $\eta'$ mass spectra.

| | $\eta_\pi$ (GeV/$c^2$) | $\omega$ (GeV/$c^2$) | $\eta'$ (GeV/$c^2$) |
|---|---|---|---|
| Signal region | (0.525, 0.560) | (0.757, 0.807) | (0.943, 0.973) |
| Sideband region | (0.497, 0.515) or (0.570, 0.587) | (0.722, 0.747) or (0.817, 0.842) | (0.918, 0.933) or (0.983,0.998) |

showers within an angle of 10° of the location of charged particles at the EMC are rejected. For $\pi^0$ and $\eta_\gamma$ reconstruction, the $\gamma\gamma$ invariant mass is required to be within $(0.115, 0.150)$ and $(0.515, 0.575)$ GeV/$c^2$, respectively. To improve $\pi^0$ and $\eta_\gamma$ momentum resolution, a kinematic fit is performed to constrain the $\gamma\gamma$ invariant mass to the appropriate world average mass [6]. The four-momenta of the $\gamma\gamma$ combinations from the kinematic fit are used in further analysis. Since there are two $\eta$ mesons in the final state of the $D^0 \to \eta'\eta$ decay, the $\pi^+\pi^-\eta$ combination with invariant mass closer to the world average $\eta'$ mass [6] is regarded as the $\eta'$ candidate. Figure 2 illustrates the distributions of the $\gamma\gamma$, $\pi^+\pi^-\pi^0$ and $\pi^+\pi^-\eta$ invariant masses for $\pi^0$ and $\eta_\gamma$, $\omega$ and $\eta_\pi$, and $\eta'$ candidates from data, after above requirements. In all cases, our nominal $\Delta E$ requirements are applied, and $M_{\rm BC}$ is required to be in the interval $(1.860, 1.870)$ GeV/$c^2$. See the next paragraph for details about the definitions of $\Delta E$ and $M_{\rm BC}$. For $\eta_\pi$, $\omega$ and $\eta'$ signals, the $\pi^+\pi^-\pi^0$ and $\pi^+\pi^-\eta$ invariant masses are required to be within signal regions as shown in Table I.

For each selected $D^0$ candidate, two variables, the energy difference $\Delta E = E_{D^0} - E_{\rm beam}$ and the beam energy constrained mass $M_{\rm BC} = \sqrt{E^2_{\rm beam}/c^4 - |\vec{p}_{D^0}|^2/c^2}$ are calculated, where $E_{\rm beam}$ is the beam energy, $E_{D^0}$ and $\vec{p}_{D^0}$ are the energy and momentum of the $D^0$ candidate in the $e^+e^-$ center-of-mass system. In the case of a correct $D^0$ candidate, $\Delta E$ and $M_{\rm BC}$ will peak around zero and the nominal $D^0$ mass [6], respectively. If multiple candidates are found only the combination with the smallest $|\Delta E|$ is kept in each single-tag mode. To suppress combinatorial background, mode-dependent $\Delta E$ requirements are imposed on the candidates. These correspond approximately to $3\sigma_{\Delta E}$ around the fitted $\Delta E$ peak, where $\sigma_{\Delta E}$ is the fitted resolution of the $\Delta E$ distribution. To obtain single-tag $D^0$ yields, we fit the $M_{\rm BC}$ distributions for each mode, as shown in Fig. 3. In these fits, the $D^0$ signal is modeled by the MC-simulated shape convolved with a Gaussian function representing the mass resolution difference between data and the MC simulation, and the combinatorial background is described by an ARGUS function [20] with endpoint fixed to 1.8865 GeV/$c^2$. The parameters of the Gaussian and ARGUS functions are determined in the fit. The resulting single-tag $D^0$ yields, $N_{\rm sig}$, are summarized in Table II.

For the decays containing an $\eta_\pi$, $\omega$ or $\eta'$ meson in the final state, the non-$\eta_\pi$, $\omega$ or $\eta'$ contribution in the $\eta_\pi$, $\omega$ or $\eta'$ signal region is estimated by using the candidate events within the invariant mass sidebands listed in Table I. To obtain the single-tag $D^0$ yields in the sideband regions, $N_{\rm sid}$ (see Table II), the corresponding $M_{\rm BC}$ distributions are fitted using a method similar to that described above. However, due to the low statistics and high backgrounds, only the parameters of the ARGUS function are left free, while the parameters of the smearing Gaussian function are fixed to the values extracted from the $M_{\rm BC}$ fit in the signal region. The non-$\pi^0$ and non-$\eta_\gamma$ contributions in the $\gamma\gamma$ invariant mass spectra are ignored since decays of the form $D^0 \to \gamma\gamma X$ are highly suppressed, and therefore any combinatoric background under the $\pi^0$ or $\eta_\gamma$ signals will not peak in $M_{\rm BC}$.

## IV. RESULTS FOR BRANCHING FRACTIONS

Detailed MC studies show that, except for the nonresonant $\eta_\pi$, $\omega$ and $\eta'$ background components, which are estimated from sideband regions, no other background processes peak in the $M_{\rm BC}$ distribution. We may thus determine the BF for the hadronic decay $D^0 \to f$ via

$$\mathcal{B}(D^0 \to f) = \frac{N_{\rm net}}{n \cdot N^{\rm tot}_{D^0\bar{D}^0} \cdot \epsilon \cdot \mathcal{B}_{\rm int}}. \quad (1)$$

Here, $N_{\rm net}$ is the net signal yield, which is $N_{\rm sig} - N_{\rm sid}$ ($N_{\rm sig}$) when a sideband subtraction is (is not) applied to the

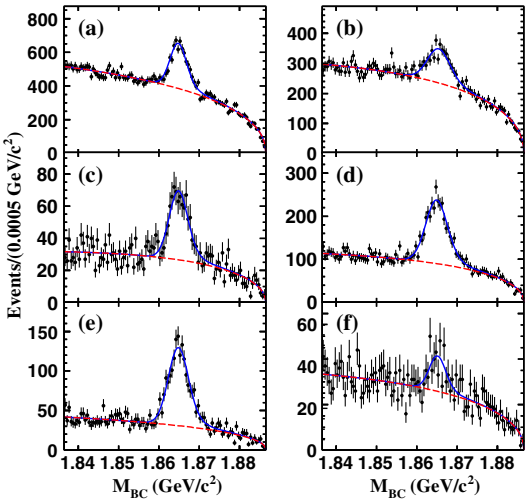


FIG. 3. Fits to the $M_{\rm BC}$ distributions of the (a) $D^0 \to \omega\eta$, (b) $D^0 \to \eta\pi^0$, (c) $D^0 \to \eta'\pi^0$, (d) $D^0 \to \eta_\gamma\eta_\gamma$, (e) $D^0 \to \eta_\pi\eta_\gamma$ and (f) $D^0 \to \eta'\eta$ candidate events in data. The points with error bars are data. The blue curves are the total fit results; the red dashed curves are the background components.

TABLE II. Summary of the singly tagged $D^0$ yields ($N_{\rm sig}$) in the signal (sideband) region in data, the detection efficiencies ($\epsilon$), the decay BFs of the intermediate particles $\pi^0$, $\eta_{(\gamma)(\pi)}$, $\omega$ and $\eta'$ ($\mathcal{B}_{\rm int}$) [6], which are not included in the detection efficiencies and the measured BFs ($\mathcal{B}$). The uncertainties are statistical only. The symbol "–" denotes that the item is not relevant.

| Decay mode | $N_{\rm sig}$ | $N_{\rm sid}$ | $\epsilon$ (%) | $\mathcal{B}_{\rm int}$ (%) | $\mathcal{B}$ ($\times 10^{-3}$) |
|---|---|---|---|---|---|
| $D^0 \to \omega\eta$ | $2961 \pm 146$ | $784 \pm 97$ | $13.77 \pm 0.19$ | 34.65 | $2.15 \pm 0.17$ |
| $D^0 \to \eta\pi^0$ | $1695 \pm 144$ | ... | $35.27 \pm 0.30$ | 38.85 | $0.58 \pm 0.05$ |
| $D^0 \to \eta'\pi^0$ | $530 \pm 48$ | $61 \pm 28$ | $14.21 \pm 0.12$ | 8.83 | $0.93 \pm 0.11$ |
| $D^0 \to \eta_\gamma\eta_\gamma$ | $2123 \pm 87$ | ... | $29.74 \pm 0.16$ | 15.45 | $2.18 \pm 0.09$ |
| $D^0 \to \eta_\pi\eta_\gamma$ | $1315 \pm 54$ | $61 \pm 29$ | $15.10 \pm 0.12$ | 17.67 | $2.22 \pm 0.11$ |
| $D^0 \to \eta'\eta$ | $170 \pm 33$ | $12 \pm 25$ | $12.01 \pm 0.10$ | 6.63 | $0.94 \pm 0.25$ |

intermediate mass spectra. The factor $n$ is four for the $D^0 \to \eta_\pi\eta_\gamma$ decay and two for other decays. The common factor of two accounts for charge conjugation, while the additional factor of two in the $D^0 \to \eta_\pi\eta_\gamma$ decay accounts for the two possible $\eta_\pi\eta_\gamma$ combinations per $D^0$ meson decay. $N^{\rm tot}_{D^0\bar{D}^0}$ is the total number of $D^0\bar{D}^0$ pairs in data, which is determined to be $(10597 \pm 28 \pm 89) \times 10^3$ [21], $\epsilon$ is the detection efficiency, and $\mathcal{B}_{\rm int}$ denotes the decay BFs of the intermediate particles $\pi^0$, $\eta_{\gamma(\pi)}$, $\omega$ and $\eta'$ [6], which are not included in the detection efficiencies. The numbers of peaking background events in the $M_{\rm BC}$ distributions are assumed to be equal between signal and sideband regions.

The detection efficiencies are estimated by analyzing signal MC events with the same procedure as data analysis, and are listed in Table II. Detailed studies show that the MC simulated events model data well.

Inserting the numbers of $N_{\rm net}$, $n$, $N^{\rm tot}_{D^0\bar{D}^0}$ [21], $\epsilon$ and $\mathcal{B}_{\rm int}$ [6] into Eq. (1), we obtain the resultant BFs shown in Table II, where the uncertainties are statistical only.

## V. SYSTEMATIC UNCERTAINTY

Sources of systematic uncertainty in the BF measurements are summarized in Table III and discussed below.

(i) $N^{\rm tot}_{D^0\bar{D}^0}$: The uncertainty of the total number of $D^0\bar{D}^0$ pairs, 0.9% [21], is considered as a systematic uncertainty for each decay.

(ii) $\pi^\pm$ *tracking and PID*: The $\pi^\pm$ tracking and PID efficiencies are studied by analyzing double-tagged hadronic $D\bar{D}$ events. The systematic uncertainty for the $\pi^\pm$ tracking and PID efficiencies each are assigned to be 1.0% per track. Tracking and PID systematics are each treated as fully correlated among themselves, but uncorrelated with each other.

(iii) $\pi^0$ *and* $\eta_{(\gamma)}$ *reconstruction*: The $\pi^0$ reconstruction efficiency is studied by analyzing double-tagged hadronic decays $D^0 \to K^-\pi^+$ and $K^-\pi^+\pi^+\pi^-$ versus $\bar{D^0} \to K^+\pi^-\pi^0$ and $K^0_S\pi^0$. The systematic uncertainties of both the $\pi^0$ reconstruction efficiency and the $\eta_{(\gamma)}$ reconstruction efficiency are found to be 2.0%.

(iv) $\omega, \eta_\pi$ *or* $\eta'$ *signal window*: The signal mass windows are widened by 2 MeV/$c^2$ for the $\omega$, $\eta_\pi$ or $\eta'$ used in $D^0 \to \omega\eta$, $\eta_\pi\eta_\gamma$. $\eta'\pi^0$ or $\eta'\eta$ decays. We then redetermine the BFs, and the resulting differences, ranging from 0.5% to 3.3%, are taken as systematic uncertainties.

(v) $\Delta E$ *requirement*: Our $\Delta E$ requirements are widened from 3 to 3.5 times the fitted width, and we recalculate the BFs. The resulting differences, ranging from 3.0% to 8.7%, are taken as systematic uncertainties.

(vi) $M_{\rm BC}$ *fit*: The uncertainties associated with the $M_{\rm BC}$ fits are estimated by comparing the nominal BFs to the measured values with alternative signal yield fits. Variations include alternative total fit ranges of (1.8335,1.8865) or (1.8395, 1.8865) GeV/$c^2$, alternative endpoints of 1.8863 or 1.8867 GeV/$c^2$ for the ARGUS background function, and changes in the detailed method used to extract the MC signal shape. The quadratic sum of changes in the BFs, ranging from 1.5% to 5.3%, are taken as the systematic uncertainties.

(vii) *Normalization of the backgrounds in signal/sideband regions (BKG normalization)*: Our nominal sideband subtraction for peaking backgrounds from nonresonant combinatorics in the $\omega$, $\eta_\pi$ and $\eta'$ spectra assumes that the equal area of the sideband and signal regions gives a correct normalization. This is investigated by using instead a scale factor obtained from fitting the corresponding $\pi^+\pi^-\pi^0$ or $\pi^+\pi^0\eta$ invariant mass spectra in data and integrating the background shape. The relative changes of the BFs, ranging from 0.4% to 1.1% are used as systematic uncertainties.

(viii) *Intermediate BFs*: The uncertainties on the quoted BFs for $\pi^0 \to \gamma\gamma$, $\eta \to \gamma\gamma$, $\omega \to \pi^+\pi^-\pi^0$, $\eta \to \pi^+\pi^-\pi^0$ and $\eta' \to \pi^+\pi^-\eta$ of 0.03%, 0.5%, 0.8%, 1.2% and 1.6% [6], respectively, are propagated as systematic uncertainties.

(ix) *MC statistics*: The uncertainties due to limited MC statistics used in determining efficiencies, varying from 0.5% to 1.3%, are included.

TABLE III. Systematic uncertainties (%) of the measured BFs, where *com* and *ind* denote the common and independent systematic uncertainties in the measured BFs for $D^0 \to \eta_\gamma\eta_\gamma$ and $D^0 \to \eta_\pi\eta_\gamma$; the symbol "–" denotes that the uncertainty is not relevant.

| Source | $D^0 \to \omega\eta$ | $D^0 \to \eta\pi^0$ | $D^0 \to \eta'\pi^0$ | $D^0 \to \eta_\gamma\eta_\gamma$ | | $D^0 \to \eta_\pi\eta_\gamma$ | | $D^0 \to \eta'\eta$ |
|---|---|---|---|---|---|---|---|---|
| | | | | *com* | *ind* | *com* | *ind* | |
| $N^{\rm tot}_{D^0\bar{D}^0}$ | 0.9 | 0.9 | 0.9 | 0.9 | ··· | 0.9 | ··· | 0.9 |
| $\pi^\pm$ tracking | 2.0 | ··· | 2.0 | ··· | ··· | ··· | 2.0 | 2.0 |
| $\pi^\pm$ PID | 2.0 | ··· | 2.0 | ··· | ··· | ··· | 2.0 | 2.0 |
| $\pi^0$ and $\eta_{(\gamma)}$ reconstruction | 4.0 | 4.0 | 4.0 | 4.0 | ··· | 4.0 | ··· | 4.0 |
| $\omega$, $\eta_\pi$ or $\eta'$ signal window | 0.5 | ··· | 3.3 | ··· | ··· | ··· | 0.9 | 1.1 |
| $\Delta E$ requirement | 3.9 | 4.8 | 7.5 | ··· | 3.1 | ··· | 3.0 | 8.7 |
| $M_{\rm BC}$ fit | 2.3 | 5.3 | 2.5 | ··· | 1.5 | ··· | 1.7 | 4.5 |
| BKG normalization | 0.5 | ··· | 1.1 | ··· | ··· | ··· | 0.4 | 0.9 |
| Quoted BF | 0.9 | 0.5 | 1.7 | 0.5 | 0.5 | 0.5 | 1.2 | 1.7 |
| MC statistics | 1.3 | 0.8 | 0.9 | ··· | 0.5 | ··· | 0.8 | 0.8 |
| Total | 6.9 | 8.3 | 9.6 | 5.4 | | 6.3 | | 11.2 |

All the individual systematic uncertainties are summarized in Table III. For the measurements of $D^0 \to \eta_\pi\eta_\gamma$ and $D^0 \to \eta_\gamma\eta_\gamma$, the systematic uncertainties are classified into common and independent parts, necessary for the proper combination of these two measurements later. For each decay, the total systematic uncertainty is the quadratic sum of the individual ones.

## VI. SUMMARY

Based on an analysis of the singly tagged events using the data sample of 2.93 fb$^{-1}$ taken at $\sqrt{s} = 3.773$ GeV with the BESIII detector, the BFs of the SCS decays $D^0 \to \omega\eta$, $\eta\pi^0$, $\eta'\pi^0$, $\eta\eta$ and $\eta'\eta$ are measured, and are summarized in Table IV. Here, the first and second uncertainties are statistical and systematic, respectively. The presented $\mathcal{B}(D^0 \to \eta\eta)$ is the combination of two individual measurements, $\mathcal{B}(D^0 \to \eta_\gamma\eta_\gamma) = (2.18 \pm 0.09 \pm 0.12) \times 10^{-3}$ and $\mathcal{B}(D^0 \to \eta_\pi\eta_\gamma) = (2.22 \pm 0.11 \pm 0.14) \times 10^{-3}$, by using the least squares method [22] and incorporating the common and independent uncertainties between the two modes as shown in Table III.

We compare the measured BFs and the world-average values, as shown in Table IV. The $\mathcal{B}(D^0 \to \omega\eta)$ is measured for the first time and its magnitude is consistent with the theoretical prediction [2–4], while the other four BFs are consistent with the world averaged values within uncertainties, and are of comparable or significantly improved ($D^0 \to \eta\eta$) precision. These measurements provide helpful experimental data to improve our understanding of SU(3)-flavor symmetry breaking effects in $D$ decays [5].

TABLE IV. Comparisons of the BFs ($\times 10^{-3}$) measured in this work and the world averaged values.

| Decay mode | This work | PDG [6] |
|---|---|---|
| $D^0 \to \omega\eta$ | $2.15 \pm 0.17 \pm 0.15$ | ··· |
| $D^0 \to \eta\pi^0$ | $0.58 \pm 0.05 \pm 0.05$ | $0.68 \pm 0.07$ |
| $D^0 \to \eta'\pi^0$ | $0.93 \pm 0.11 \pm 0.09$ | $0.90 \pm 0.14$ |
| $D^0 \to \eta\eta$ | $2.20 \pm 0.07 \pm 0.06$ | $1.67 \pm 0.20$ |
| $D^0 \to \eta'\eta$ | $0.94 \pm 0.25 \pm 0.11$ | $1.05 \pm 0.26$ |

## ACKNOWLEDGMENTS

The BESIII collaboration thanks the staff of BEPCII and the IHEP computing center for their strong support. This work is supported in part by National Key Basic Research Program of China under Contract No. 2015CB856700; National Natural Science Foundation of China (NSFC) under Contracts Nos. 11235011, 11305180, 11775230, 11335008, 11425524, 11625523, 11635010; the Chinese Academy of Sciences (CAS) Large-Scale Scientific Facility Program; the CAS Center for Excellence in Particle Physics (CCEPP); Joint Large-Scale Scientific Facility Funds of the NSFC and CAS under Contracts Nos. U1332201, U1532257, U1532258; CAS under Contracts Nos. KJCX2-YW-N29, KJCX2-YW-N45, QYZDJ-SSW-SLH003; 100 Talents Program of CAS; National 1000 Talents Program of China; INPAC and Shanghai Key Laboratory for Particle Physics and Cosmology; German Research Foundation DFG under Contracts Nos. Collaborative Research Center CRC 1044, FOR 2359; Istituto Nazionale di Fisica Nucleare, Italy; Joint Large-Scale Scientific Facility Funds of the NSFC and CAS; Koninklijke Nederlandse Akademie van Wetenschappen (KNAW) under Contract No. 530-4CDP03; Ministry of Development of Turkey under Contract No. DPT2006K-120470; National Natural Science Foundation of China (NSFC) under Contract No. 11505010; National Science and Technology fund; The Swedish Research Council; U.S. Department of Energy under Contracts Nos. DE-FG02-05ER41374, DE-SC-0010118, DE-SC-0010504, DE-SC-0012069; University of Groningen (RuG) and the Helmholtzzentrum fuer Schwerionenforschung GmbH (GSI), Darmstadt; WCU Program of National Research Foundation of Korea under Contract No. R32-2008-000-10155-0.

[1] B. Bhattacharya and J. L. Rosner, Phys. Rev. D **81**, 014026 (2010).
[2] H. Y. Cheng and C. W. Chiang, Phys. Rev. D **81**, 074021 (2010).
[3] H. Y. Cheng, C. W. Chiang, and A. L. Kuo, Phys. Rev. D **93**, 114010 (2016).
[4] Q. Qin, H. Li, C. D. Lü, and F. S. Yu, Phys. Rev. D **89**, 054006 (2014).
[5] W. Kwong and S. P. Rosen, Phys. Lett. B **298**, 413 (1993); Y. Grossman and D. J. Robinson, J. High Energy Phys. 04 (2013) 67.
[6] C. Patrignani *et al.* (Particle Data Group), Chin. Phys. C **40**, 100001 (2016).
[7] M. Artuso *et al.* (CLEO Collaboration), Phys. Rev. D **77**, 092003 (2008).
[8] H. Mendez *et al.* (CLEO Collaboration), Phys. Rev. D **81**, 052013 (2010).
[9] M. Ablikim *et al.* (BESIII Collaboration), Chin. Phys. C **37**, 123001 (2013); Phys. Lett. B **753**, 629 (2016).
[10] M. Ablikim *et al.* (BESIII Collaboration), Phys. Rev. D **91**, 112015 (2015).
[11] M. Ablikim *et al.* (BESIII Collaboration), Phys. Rev. Lett. **116**, 082001 (2016).
[12] M. Ablikim *et al.* (BESIII Collaboration), Nucl. Instrum. Methods Phys. Res., Sect. A **614**, 345 (2010).
[13] S. Agostinelli *et al.* (GEANT4 Collaboration), Nucl. Instrum. Methods Phys. Res., Sect. A **506**, 250 (2003).
[14] S. Jadach, B. F. L. Ward, and Z. Was, Comput. Phys. Commun. **130**, 260 (2000); Phys. Rev. D **63**, 113009 (2001).
[15] E. A. Kureav and V. S. Fadin, Yad. Fiz. **41**, 733 (1985) [Sov. J. Nucl. Phys. **41**, 466 (1985)].
[16] E. Richter-Was, Phys. Lett. B **303**, 163 (1993).
[17] D. J. Lange, Nucl. Instrum. Methods Phys. Res., Sect. A **462**, 152 (2001); R. G. Ping, Chin. Phys. C **32**, 599 (2008).
[18] K. Nakamura *et al.* (Particle Data Group), J. Phys. G **37**, 075021 (2010) and 2011 partial update for the 2012 edition.
[19] J. C. Chen, G. S. Huang, X. R. Qi, D. H. Zhang, and Y. S. Zhu, Phys. Rev. D **62**, 034003 (2000).
[20] H. Albrecht *et al.* (ARGUS Collaboration), Phys. Lett. B **241**, 278 (1990).
[21] D. Toth (for BESIII Collaboration), presented at APS 551 April Meeting 2014, Savannah, Georgia, US, April 5-8, 2014. The number of $D^0\bar{D}^0$ pairs has further been corrected for quantum correlation effects (unpublished).
[22] J. Mandel, *The Statistical Analysis of Experimental Data* (Dover Publications, New York, 1964).